

Article

The Effect of Data Skewness on the LSTM-Based Mooring Load Prediction Model

Hangyu Chen ¹, Yinglei Bu ², Kun Zong ^{1,3}, Limin Huang ^{4,5,*} and Wei Hao ¹

¹ College of Shipbuilding Engineering, Harbin Engineering University, Harbin 150001, China

² Marine Design & Research Institute of China, Shanghai 200011, China

³ System Engineering Research Institute, China State Shipbuilding Corporation, Beijing 100036, China

⁴ Qingdao Innovation and Development Base of Harbin Engineering University, Harbin Engineering University, Qingdao 266000, China

⁵ Qingdao Innovation and Development Center of Harbin Engineering University, Qingdao 266000, China

* Correspondence: huanglimin@hrbeu.edu.cn

Abstract: The working condition of the floating platform will be affected by wind and waves in the marine environment. Therefore, it is of great importance to carry out real-time prediction research on the mooring load for ensuring the normal operation of the floating platform. Current researches have focused on the real-time prediction of mooring load using the machine learning method, but most of the studies are about the application and generalization analysis of different models. There are few studies on the influence of data distribution characteristics on prediction accuracy. In view of the above problems, this paper investigates the effect of data skewness on the prediction performance for the deep learning model. The long short-term memory (LSTM) neural network is applied to construct the mooring load prediction model. The numerical simulation datasets of the deep water semi-submersible platform are employed in model training and data analysis. The prediction performance of the model is preliminarily verified based on the simulation results. Meanwhile, the distribution characteristics of mooring load data under different sea states are analyzed and a skewness processing method based on the Box-Cox Transformation (BCT) is proposed. The effect of data skewness on prediction accuracy is further investigated. The comparison results indicate that reducing the mooring load data skewness can effectively improve the prediction accuracy of LSTM model.

Keywords: mooring load of floating platform; LSTM model; data skewness analysis; Box-Cox Transformation; numerical simulation verification



Citation: Chen, H.; Bu, Y.; Zong, K.; Huang, L.; Hao, W. The Effect of Data Skewness on the LSTM-Based Mooring Load Prediction Model. *J. Mar. Sci. Eng.* **2022**, *10*, 1931. <https://doi.org/10.3390/jmse10121931>

Academic Editors: Baran Yeter, Yordan Garbatov and Joško Parunov

Received: 31 October 2022

Accepted: 2 December 2022

Published: 7 December 2022

Publisher's Note: MDPI stays neutral with regard to jurisdictional claims in published maps and institutional affiliations.



Copyright: © 2022 by the authors. Licensee MDPI, Basel, Switzerland. This article is an open access article distributed under the terms and conditions of the Creative Commons Attribution (CC BY) license (<https://creativecommons.org/licenses/by/4.0/>).

1. Introduction

With the increasing demand for oil and gas resources in the deep sea, the applications of semi-submersible, FPSO, and other floating platforms have become more extensive [1]. The platform will be submitted to six-degree-of-freedom (6-DOF) motions under the action of waves. The low-frequency drift motions and 1st order motions will cause the load of the mooring system. Under severe environmental conditions, the mooring system will suffer from extreme loads, which may cause the failure of the platform system, leading to serious consequences, such as economic loss, casualties, and environmental pollution. Therefore, the study of mooring load prediction is of great significance for ensuring the safe operation of the platform.

For the study of the dynamic response of mooring systems, the Finite Element Analysis (FEA) based on rod theory is widely used in the field of marine technology. This method was first presented to solve the static and dynamic problems of three-dimensional (3D) nonlinear mooring lines [2]. On this basis, Webster [3] considered the deformation of mooring lines under extreme tension and applied it to the coupling analysis of the platform system. After that, an improved algorithm was proposed to solve 2D and 3D problems, which takes into account the seabed force and the elasticity of the mooring line [4]. At

present, FEA is an essential numerical method for the prediction of mooring load, but it usually needs little time steps and delicate grid discretion to obtain the stable response of the structure, which takes a long computing time. In addition, the FEA method is often used in the design stage and has limitations of applying in the real-time prediction.

Therefore, researchers have focused on the development of more effective prediction methods and some scholars tried to establish mathematical models to associate the dynamic response of the slender with its motions. Sagrilo et al. [5] proposed a polynomial model to express the heave motion of the flexible riser under the external excitation. Pascoal et al. [6] put forward another polynomial model to represent the response of the mooring system to lateral motion. Gobat and Grosenbaugh [7] presented an empirical model of the dynamic tension change of the mooring cable caused by the vertical movement measured at the top connection. They expressed the standard deviation of the top tension as the sum of inertial force and drag force. Li et al. [8] established a hydrodynamic parameters database of FPSO under different loading conditions and used the linear interpolation method to make a quick prediction of mooring force. Liu et al. [9] carried out a numerical study of the hydrodynamic characteristics of a semisubmersible aquaculture facility and verified the simulation results through experimental data. Although this method does not need to consider the complex coupling analysis of the platform-mooring system, the construction of the database still requires lots of preliminary calculations, which takes a long time.

With the rapid development of artificial intelligence technology in recent years, many studies have been carried out in various fields combined with machine learning methods [10–12]. Considering the advantages of machine learning in fitting nonlinear systems, it was generally applied in the analysis of offshore platform systems. Mazaheri et al. [13] used the Artificial Neural Network (ANN) to analyze the seakeeping performance of a turret-moored FPSO and further studied the platform response under extreme sea conditions [14]. Guarize et al. [15] applied the hybrid ANN-FEA model for the prediction of dynamic top tension of mooring lines. The prediction results showed good agreement with the FEA results, and the computational time was reduced by about 20 times. Pina et al. [16] used the hybrid method of dynamic autoregressive model and ANN model to predict the top tension of risers and obtained good results. Cortina et al. [17] further studied the application of ANN to the fatigue analysis of steel risers under wave action, and compared the results with the FEA method, the prediction errors of the two methods are close. Kim et al. [18] presented a NARX-based Volterra model to predict the dynamic response of the FPSO mooring system. The results demonstrated the accuracy and feasibility of the NARX model in mooring load prediction. Zhao et al. [19] proposed a prediction model of structural stress and deformation of fish cage based on the ANN model. Bi et al. [20] studied the ANN-based structural failure prediction of high-density polyethylene offshore net cages in typhoon waves, which provided an efficient method to forecast the damage levels under extreme environmental conditions.

In order to improve the practical engineering application of neural network models, many scholars have carried out the research on hybrid models to improve the prediction accuracy. The wavelet analysis method and the empirical model decomposition (EMD) method are widely used in engineering [21–23]. Pina et al. [24,25] presented a surrogate model combining the Wavelet Network (WN) with the ANN and respectively applied the model for the analysis of slender offshore structures and floating production systems. Meanwhile, some scholars investigated the prediction ability of the neural network model for unknown sea states. Sidarta et al. [26] proposed an ANN-based prediction model of mooring load and analyzed the prediction results under different sea conditions. Qiao et al. [27] applied the LSTM model for the real-time prediction of mooring lines and verified the prediction accuracy under unknown sea conditions, including new current directions, significant wave heights and wave periods. However, the above studies only directly use various models to analyze the prediction effect under different conditions, but ignore the distribution characteristics of the data itself. Combined with the data character-

istics, carrying out the data preprocessing research can also effectively improve the model prediction accuracy.

In this paper, a real-time prediction model for mooring loads based on the LSTM neural network is constructed, which takes the 6-DOF motion of the platform as input and produces the mooring lines top tension. The prediction accuracy is verified under different sea conditions. Meanwhile, based on the constructed model, this paper mainly investigates the influence of mooring load data skewness on prediction performance. An innovative data preprocessing method based on Box-Cox Transformation (BCT) is proposed to improve prediction accuracy.

The rest of the paper is organized as follows. Section 2 explains the principle of dynamic coupling analysis between the platform and the mooring system. Section 3 presents the structure of the LSTM-based prediction model and the preprocessing method of data skewness. Section 4 introduces the definition of the skewness and proposes a data skewness processing method. Section 5 introduces the numerical simulation results of the validation platform model and the analysis of data skewness characteristics. Section 6 verifies the accuracy of the proposed model and further analyzes the prediction performance with the data skewness preprocessing method. In the final part, some concluding remarks are made.

2. Dynamic Coupling Model of Floating Platform and Mooring System

The deep-sea floating platform is mainly composed of the main body and the mooring system. In the marine environment, the mooring load and the platform motion are coupled with each other, which forms a complex coupling dynamic system. The asynchronous coupling algorithm [28] is widely used in the coupled system analysis. This method treats the floating platform and the mooring lines as two independent systems, which are connected by the same displacement and interaction force at the junction.

For the platform body, the hydrodynamic load can be obtained by integrating along the wet surface.

$$F_{\omega} = -\rho \iint_{S_H} \frac{\partial}{\partial t} [(\Phi_0 + \Phi_D + \Phi_j)e^{-i\omega t}] n_j ds \tag{1}$$

where ρ is the density of water, n_j is the normal vector of the wet surface, Φ_0 , Φ_D and Φ_j are incident potential, radiated potential, and diffracted potential.

Considering the slender components on the platform, the hydrodynamic load of slender rods can be calculated by the Morison formula.

$$F = \int_{z_1}^{z_2} \rho \frac{\pi D^2}{4} C_M a dz + \int_{z_1}^{z_2} \frac{\rho}{2} C_D D |u| u dz \tag{2}$$

where ρ is the density of water, D is the diameter of slender rods, u and a are horizontal velocity and acceleration at the center of slender rods, C_M and C_D are inertia coefficient and drag coefficient.

Considering the coupled relationship between the platform body and mooring system, the 6-DOF motion equation on the time domain can be expressed as follows:

$$(M + m)\ddot{x}(t) + \int_{-\infty}^t K(t - \tau)\dot{x}(\tau)d\tau + Cx(t) = F(t) + F_{moor}(t) \tag{3}$$

where M is the generalized mass matrix, m is the added mass matrix, $K(t - \tau)$ is the delay function matrix, C is the total stiffness matrix, $F(t)$ is the generalized fluid force matrix, $F_{moor}(t)$ is the mooring force matrix.

The mooring force is calculated by the current position of the platform, and the position of the platform at the next moment is affected by the calculated mooring force. In this way, the motion of the platform and the force of mooring lines can be obtained through iterative calculation.

3. LSTM-Based Mooring Load Prediction Model

3.1. LSTM Neural Network

The long short-term memory (LSTM) neural network is a special kind of recurrent neural network (RNN), which includes the time cycle structure in deep learning and can accurately model the time series data [29]. Compared with the RNN, the LSTM model introduces three kinds of gates to control the information transmission between neurons, which can effectively avoid the gradient vanishing problem of the RNN. The original LSTM architecture is shown in Figure 1.

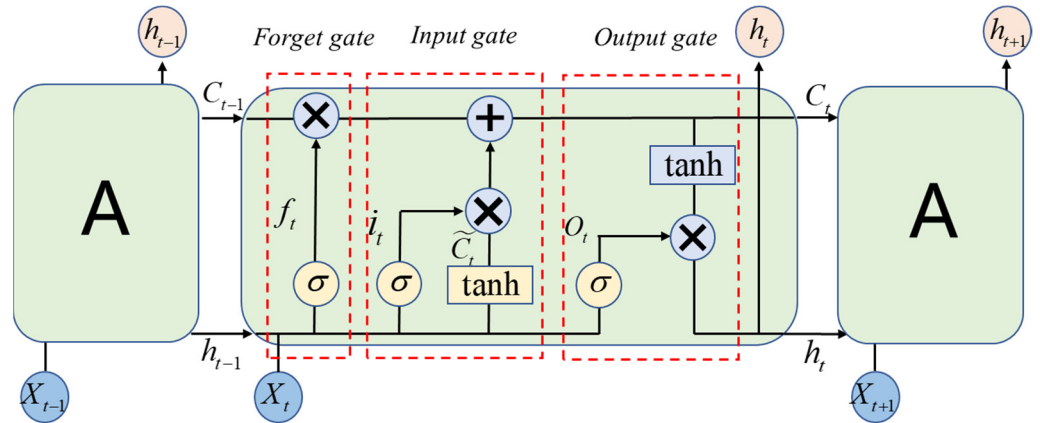


Figure 1. LSTM structure.

As shown in Figure 1, a single LSTM neuron includes three gate control units: forget gate, input gate, and output gate. The forget gate determines the information abandoned from the neuron, which reflects the influence of historical information on the state value of the current neuron.

The input gate is used to control the effect of the current input data on the state value of the neuron. It receives the information from the previous hidden state and current input first and then calculates the information that needs to be updated. The updating equations can be summarized as follows:

$$f_t = \sigma(W_f[X_t, h_{t-1}] + b_f) \tag{4}$$

$$i_t = \sigma(W_i[X_t, h_{t-1}] + b_i) \tag{5}$$

$$\tilde{C}_t = \tanh(W_c[X_t, h_{t-1}] + b_c) \tag{6}$$

$$C_t = f_t C_{t-1} + i_t \tilde{C}_t \tag{7}$$

where h_{t-1} is the output of the previous neuron, X_t is the input vector, σ is the activation function, W_f , W_i and W_c are weight matrices, b_f , b_i and b_c are bias matrices. C_{t-1} and C_t represent the information storage state of the previous neuron and the current neuron, respectively.

The output gate decides the output data of the current neuron. The activation function is computed based on the value of the output gate and the current cell state.

$$o_t = \sigma(W_o[X_t, h_{t-1}] + b_o) \tag{8}$$

$$h_t = o_t \tanh(C_t) \tag{9}$$

where W_o is the weight coefficient, b_o is the bias of o_t , h_t is the output of current neuron.

3.2. The Structure of Mooring Load Prediction Model

There is a non-linear mapping relationship between the platform motion and the mooring load. The relationship can be described by complicated hydrodynamic equations, which are widely used in the traditional prediction methods. In fact, there is a strong correlation between motion time series and tension time series. As mentioned in Section 3.1, the LSTM neural network is used to consider the correlation of data. Therefore, the LSTM model is developed to predict the response of the mooring line by the known motion response of the platform in this study.

The framework of the LSTM-based prediction model is shown in Figure 2, where FC means fully connected and Act means activation. The LSTM model constructed in this paper adopts a single hidden layer with 16 neurons. The input layer is the 6-DOF motion matrix of the platform, and the output layer is the tension response of mooring lines. The Adam optimizer is used to train the model parameters and the hyperbolic tangent function is used as the activation function in the hidden layer. The loss function selects the mean square error (MSE).

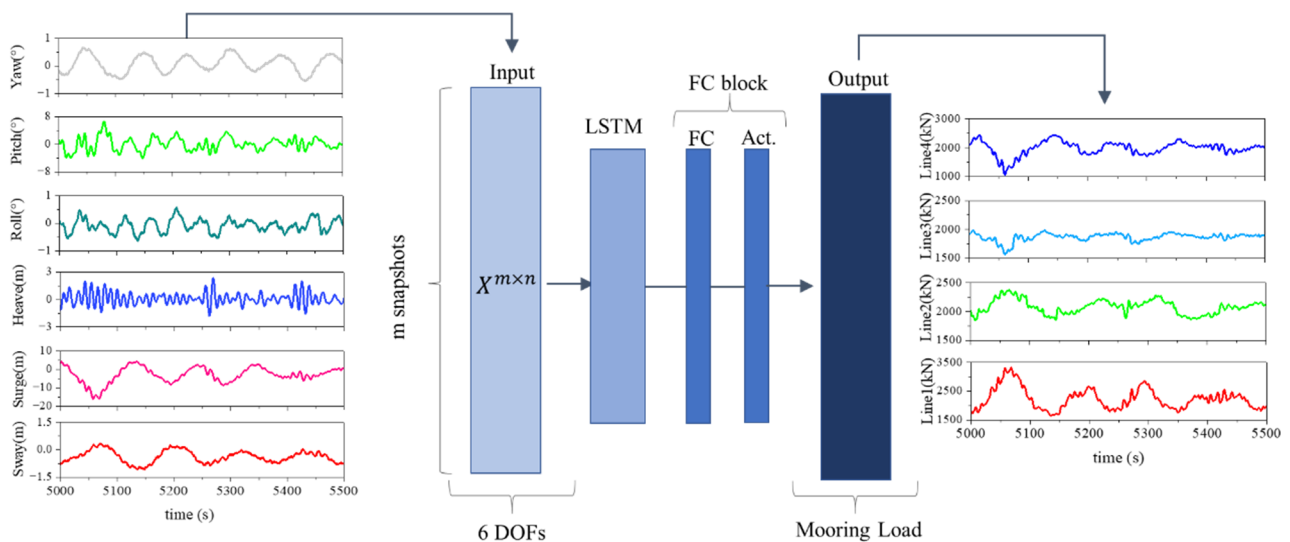


Figure 2. Illustration of the LSTM-based mooring load prediction model.

The training of the LSTM neural network consists of the following steps: firstly, the original input data is delivered into the neural network and there is an original weight matrix of the model used to calculate the output results; secondly, the computed results are compared to the desired actual output data value and the generated error is calculated by the loss function; thirdly, the generated error is distributed to each unit in each layer in the process of back propagation, and the error value of each unit is obtained; and finally, adjust the weight matrix to minimize the generated total error to match the accuracy requirement. Figure 3 shows the generated total error in each training epoch. It can be seen that the error between the train data and validation data is getting close with the increase of training epochs, which means that this LSTM model is generalized well.

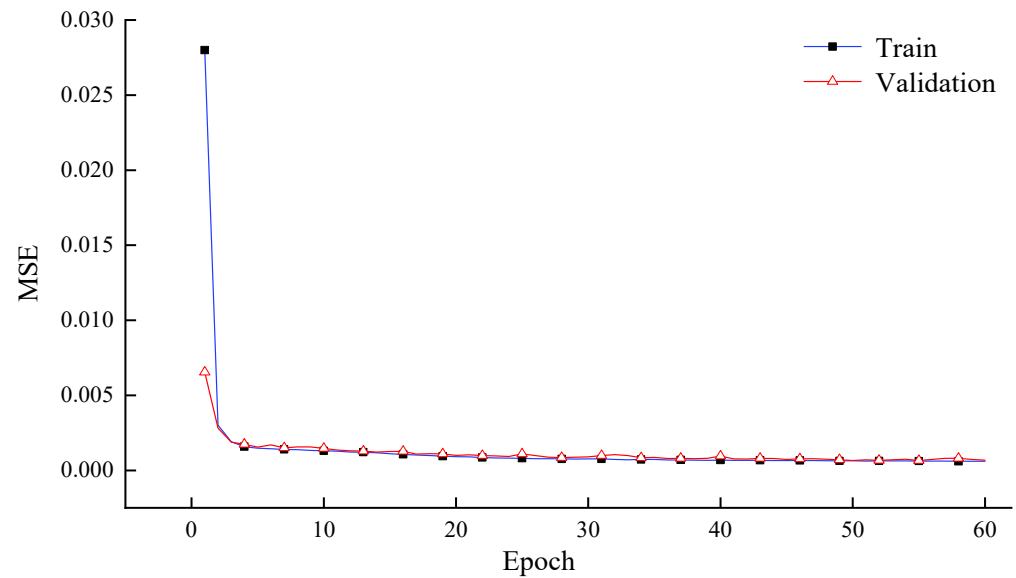


Figure 3. Training performance of the LSTM network in terms of MSE of the training and validation partitions.

4. Skewness Analysis and Pre-Processing Method

4.1. Data Skewness

Skewness is a measure of the asymmetry of data distribution. It is a statistical tool with the advantage of being independent of the mean of the data. The skewed distribution is compared with the normal distribution, where the normal distribution is symmetrical and the skewness is zero. A systematical study of skewness began with Karl Pearson [30] who first investigated the property of skewness of different types of statistics. That was followed by Groeneveld et al. [31] and Rayner et al. [32], giving a summary of skewness property of different distributions including Gamma distribution, log-logistic distribution, log-normal distribution and Weibull distribution. The formula of data skewness is defined as:

$$skewness = \frac{\frac{1}{n} \sum_{i=1}^n (x_i - X_{mean})^3}{\left(\sqrt{\frac{1}{n} \sum_{i=1}^n (x_i - X_{mean})^2} \right)^3} \tag{10}$$

where x_i is the data set, X_{mean} is the mean value of the data set.

The negative skewness reveals that more data is distributed on the left side of the data mean, while positive reveals that more data is distributed on the right side of the mean. As shown in Table 1, the values of skewness reflect the degree of data asymmetry.

Table 1. The relationship between data distribution and skewness.

Data Distribution	Skewness
Symmetric distribution	-0.5~0.5
Moderate asymmetry	-0.5~-1.0 & 0.5~1.0
High asymmetry	<-1.0 & >1.0

4.2. Box-Cox Transformation

The Box-Cox Transformation (BCT), which was originally proposed by Box and Cox (1964), is commonly used to normalize the data distribution. The calculation formula is defined as:

$$F(y_i, \lambda) = \begin{cases} \frac{y_i^\lambda - 1}{\lambda} & \text{if } \lambda \neq 0 \\ \ln(y_i) & \text{if } \lambda = 0 \end{cases} \quad (11)$$

where y_i is the variable, λ is a hyper-parameter.

Compared with the log transformation, BCT can be applied to normalize the data distribution with different skewness and it avoids the singularity of the log transformation when the data is approaching zero. Thus, the BCT is selected as the normalization method for platform motion and mooring load data in this paper.

4.3. Data Skewness Processing Method

Most of algorithms in machine learning often assume that the variables obey the normal distribution. When the raw data has a large skewness, the training process of deep learning models will be affected, resulting in the reduction of prediction accuracy. Aiming at the above problems, this paper proposes a data processing method based on the BCT for the training process of mooring load prediction model, which is called the BCT-based LSTM model.

Typically, the input and output data have different units and proportions. Thus, we firstly need to normalize the platform motion data and the mooring line tension data in the interval [0, 1]. The calculation process is as follows:

$$\bar{x} = \frac{x - x_{\min}}{x_{\max} - x_{\min}} \quad (12)$$

where \bar{x} is the normalized data. x is the input sequence. x_{\max}, x_{\min} represents the maximum and minimum values in the input sequence, respectively.

Secondly, considering the BCT requires data to be positive, the data shifting is necessary for the pre-processing steps. In this paper, the positive shift is realized by adding a positive constant to the normalized data. Then, after the Box-Cox Transformation, the data is converted to the normal distribution and can be used as samples for model training.

To compare the predicted mooring load with numerical simulation results, the corresponding inverse transformations are required as the data post-processing. As shown in Figure 4, the Box-Cox Inverse Transformation (BCIT) is firstly carried out according to the following formula:

$$y_i = \begin{cases} (1 + \lambda F(y_i, \lambda))^{\frac{1}{\lambda}} & \text{if } \lambda \neq 0 \\ \exp(F(y_i, \lambda)) & \text{if } \lambda = 0 \end{cases} \quad (13)$$

where y_i represents the inverse transformed mooring load after the BCIT. $F(y_i, \lambda)$ is the mooring load predicted by the LSTM model. λ is the hyper-parameter, which needs to be consistent in the process of the BCT and the BCIT.

After the BCIT, the data inverse shift is necessary for following steps. The constant added in the process of positive shift needs to be subtracted at this step. After the above post-processing steps, now the predicted mooring load data has been restored in the interval [0, 1]. To compare with the original simulation results, the inverse normalization of datasets is further required, which can be realized by the following formula:

$$x = \bar{x}(x_{\max} - x_{\min}) + x_{\min} \quad (14)$$

where x is the inverse normalized mooring load data. \bar{x} represents the data after the inverse shift. x_{\max} and x_{\min} are consistent with the maximum and minimum values in the input sequence.

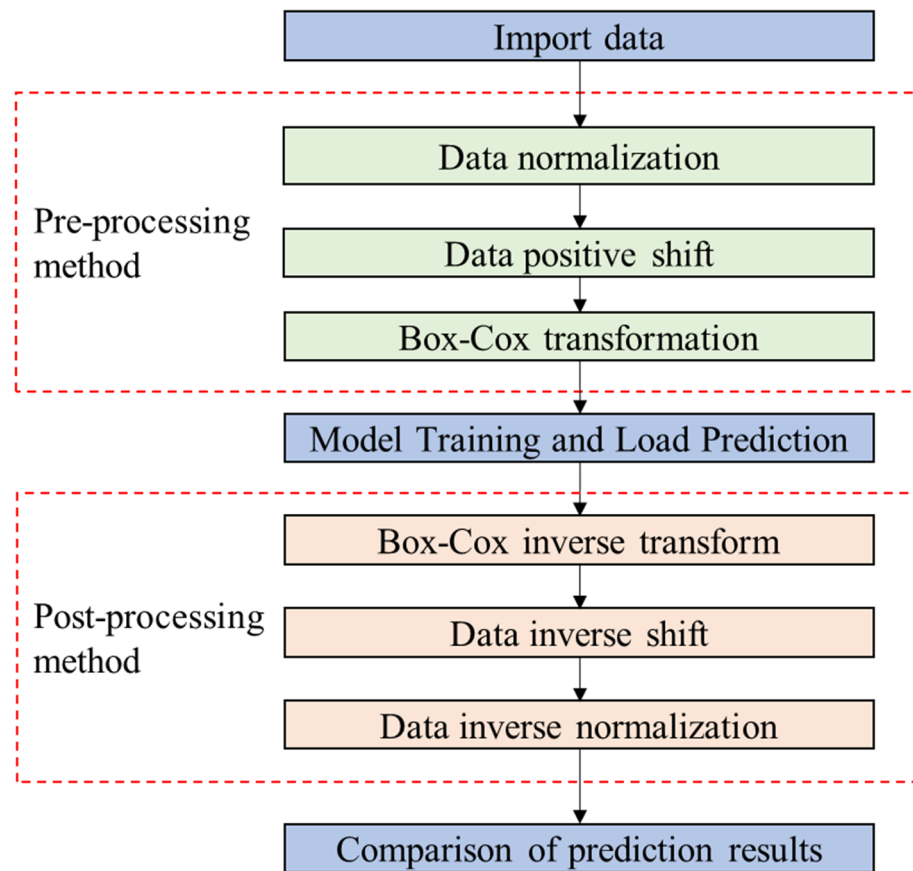


Figure 4. The flow of data processing method.

Through the above process, the effect of data skewness on the model prediction accuracy can be investigated.

5. Data Sets of the Floating Platform

5.1. Geometric Model

A deep water semi-submersible platform is employed as a case study to verify the prediction accuracy of the proposed model. The platform system is composed of two pontoons, four columns, and eight mooring lines. The primary geometric details of the floating platform are presented in Table 2. The mooring lines are symmetrically arranged and a full platform-mooring system is shown in Figure 5. The mooring line is divided into the top chain, wire, and the bottom chain three segments. The main properties of mooring lines are listed in Table 3.

Table 2. Main characteristic of platform.

Parameter	Value	Parameter	Value
Length of pontoon (m)	104.5	Longitudinal distance of columns (m)	55
Breadth of pontoon (m)	16.5	Molded depth of deck (m)	8
Height of pontoon (m)	10.05	Draft (m)	17.5
Length of column (m)	15.5	Displacement (t)	42,710
Breadth of column (m)	15.5	Pitch radius of gyration (m)	34
Height of column (m)	19.5	Roll radius of gyration (m)	32.5
Horizontal distance between columns (m)	54	Yaw radius of gyration (m)	37.5

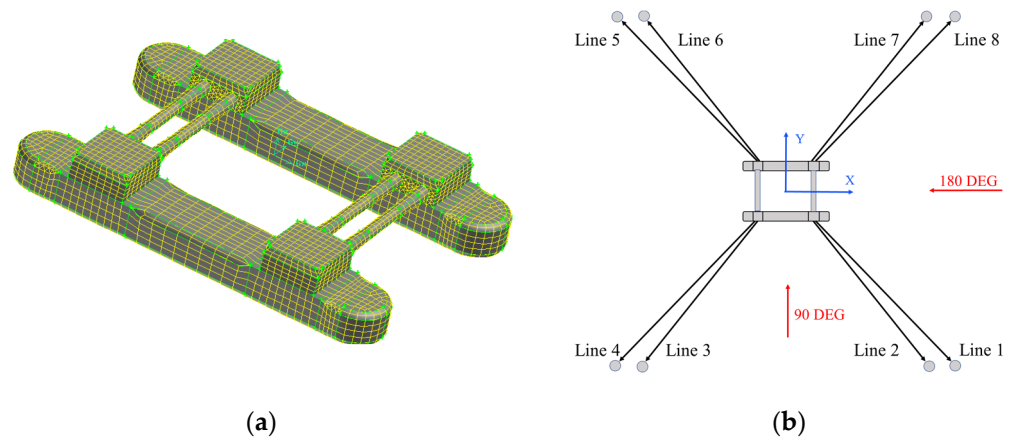


Figure 5. Schematic of semi-submersible platform and mooring system model. (a) Platform model; (b) schematic plan of mooring lines.

Table 3. Main parameters of mooring lines.

Segment	Length (m)	Elastic Modulus (Pa)	Density (kg/m ³)	Displacement Volume of Unit Length (m ³)	Cross Section Area (m ²)	Diameter (m)
Top chain	20	2.0×10^{11}	7800	0.175	0.175	0.25
Wire	280	2.0×10^{11}	7800	0.0229	0.0229	0.225
Bottom chain	900	2.0×10^{11}	7800	0.175	0.175	0.25

5.2. Numerical Simulation Data Sets

In this paper, the numerical simulation of the semi-submersible platform is carried out by using the self-developed software ‘Offshore Platform Motions in Operation Condition Virtual Test’ of Harbin Engineering University, which is based on the Taylor expansion boundary element method (TEBEM) and the simulation accuracy of the software is verified to be equivalent to that of AQWA [33,34]. The motion response of the platform and the corresponding mooring line tensions are computed under different work conditions. As shown in Figure 6, the JONSWAP spectrum was adopted to represent the sea surface elevation. The simulated wave environments select sea state 4–7 and corresponding wave parameters are shown in Table 4. The wave direction selects 180° and the water depth is set as the infinite depth.

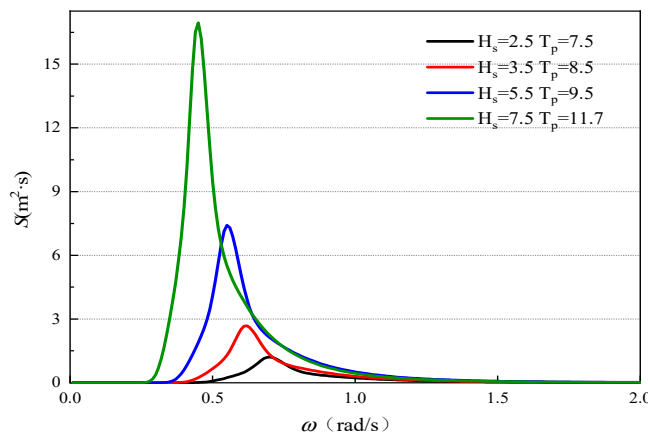


Figure 6. Wave spectrum.

Table 4. Wave spectrum parameters for numerical simulation.

Sea State	Significant Height (m)	Spectrum Peak Period (s)	Spectrum Peak Factor γ	Low Cut-Off Frequency (Rad/s)	High Cut-Off Frequency (Rad/s)
4	2.5	7.5	2.3	0.2	2.0
5	3.5	8.5	2.3	0.2	2.0
6	5.5	9.5	2.3	0.2	2.0
7	7.5	11.7	2.3	0.2	2.0

For above set sea conditions, the simulation time duration is 3 h and the time interval selects 0.32 s. Some simulated platform motion and mooring lines tension are shown in Figure 7.

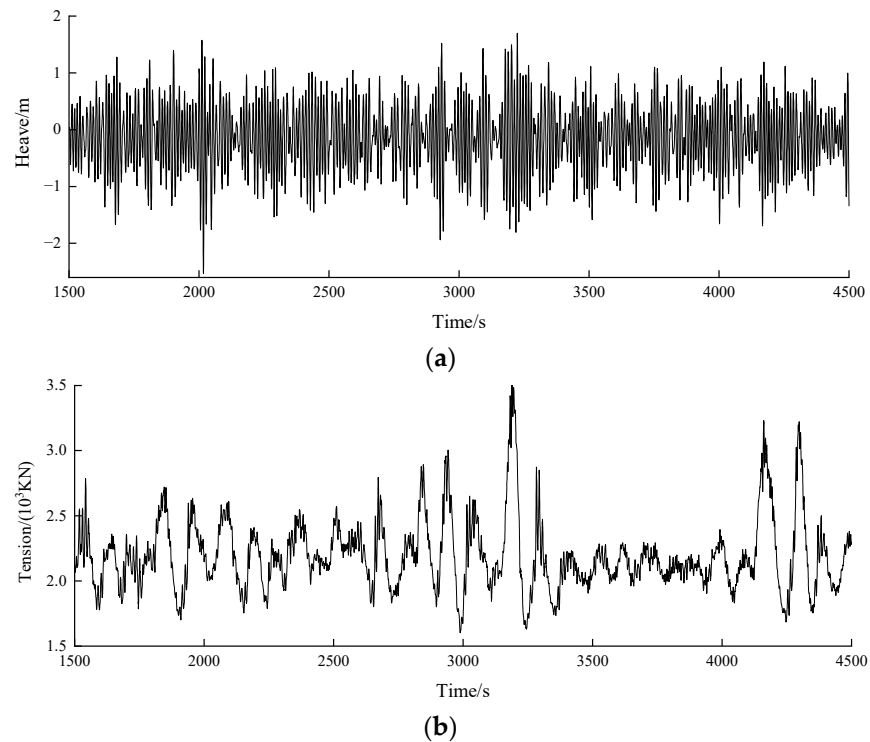


Figure 7. Part of simulated results in sea state 7. (a) The heave motion of platform in sea state 7; (b) the top tension of line #1 in sea state 7.

5.3. The Skewness Analysis of Mooring Load Data

With the change of sea conditions, the data distribution characteristics of mooring load will be influenced. To investigate the skewness of mooring load data under different sea states, this section selects line 1 as the example to carry out the statistical analysis. The distribution map from sea states 4–7 is shown in Figure 8.

As shown in Figure 8, the distribution range of mooring load gradually increases with the increase of sea states. The mooring data changes from (1800 KN, 2200 KN) of sea state 4 to (1500 KN, 4000 KN) of sea state 7. Meanwhile, the data gradually changed from symmetrical distribution (sea state 4, skewness = 0.108) to moderate asymmetry (sea state 5, skewness = 0.666) and then to high asymmetry (sea state 6 and 7, skewness = 1.148, 1.274). The above results show that with the increase of sea state, the data distribution characteristics of mooring load become more complex, which increasingly deviates from the normal distribution. That is because with the increase of sea state, the nonlinear coupling relationship between platform motion and mooring load is gradually enhanced, which no longer satisfies some linear assumptions and resulting in obvious changes in data distribution characteristics.

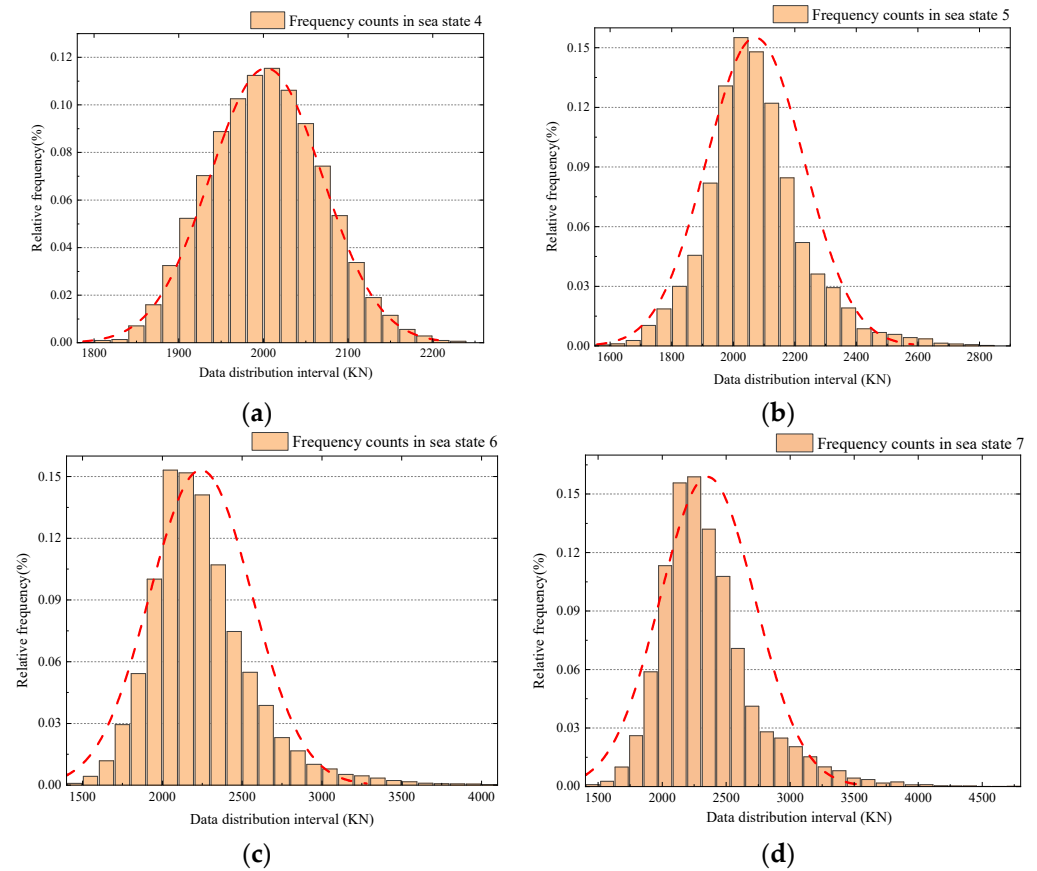


Figure 8. Frequency counts of line 1 in different sea states. (a) Frequency counts in sea state 4 (skewness = 0.108); (b) frequency counts in sea state 5 (skewness = 0.666); (c) frequency counts in sea state 6 (skewness = 1.148); and (d) frequency counts in sea state 7 (skewness = 1.274).

6. Results and Discussions

6.1. Error Assessment

In engineering, it is often concerned about whether the maximum tension of the mooring lines will exceed the stress limit, which leads to the failure of the structure. Therefore, this paper applies the extreme value error E_{max} for the statistical comparison of the maximum load error between the LSTM model prediction results and the numerical simulation results. Meanwhile, the LSTM is a time series prediction approach. To evaluate the prediction accuracy of the overall time series, the root-mean-squared error (RMSE) is selected as one of the assessment errors.

$$E_{max} = \left(\frac{y_{actu_max} - y_{pred_max}}{y_{actu_max}} \right) \times 100\% \tag{15}$$

$$RMSE = \sqrt{\frac{1}{m} \sum_{i=1}^m (y_i^{pred} - y_i^{actu})^2} \tag{16}$$

where y_{actu_max} and y_{pred_max} are the maximum value of the numerical simulation results and the LSTM model prediction results, respectively; y_i^{actu} and y_i^{pred} are the numerical simulation value and the LSTM model prediction value, respectively; m denotes the number of samples used to test the prediction.

6.2. The Valiadation of LSTM-Based Mooring Load Prediction Model

In order to preliminarily verify the prediction performance of the LSTM-based mooring load prediction model proposed in this paper, this section selects the raw data of numerical

simulation results as the training data and test data. The validation conditions include sea states 4 to 7 and the wave direction is 180° . The time length of numerical simulation data is 3 h, and the time interval is 0.32 s. The 0–7200 s time histories are chosen as the training set to make sure that the prediction model can be well trained with the sufficient training data, and the rest are set as the test set.

Under the head sea conditions, the 6-DOF motion time series of the platform are applied as the input of the LSTM model. Because the mooring lines are symmetrically arranged, the output results just need to consider the top tension of the four mooring lines, which are line #1, line #2, line #3, and line #4. The line #1 is selected as the example to display the prediction results under different sea states. The comparison between numerical simulation results and the forecasting results is shown in Figure 9. To observe the fitting performance between forecast results and numerical results conveniently, the time window selects 1000 s for comparative analysis.

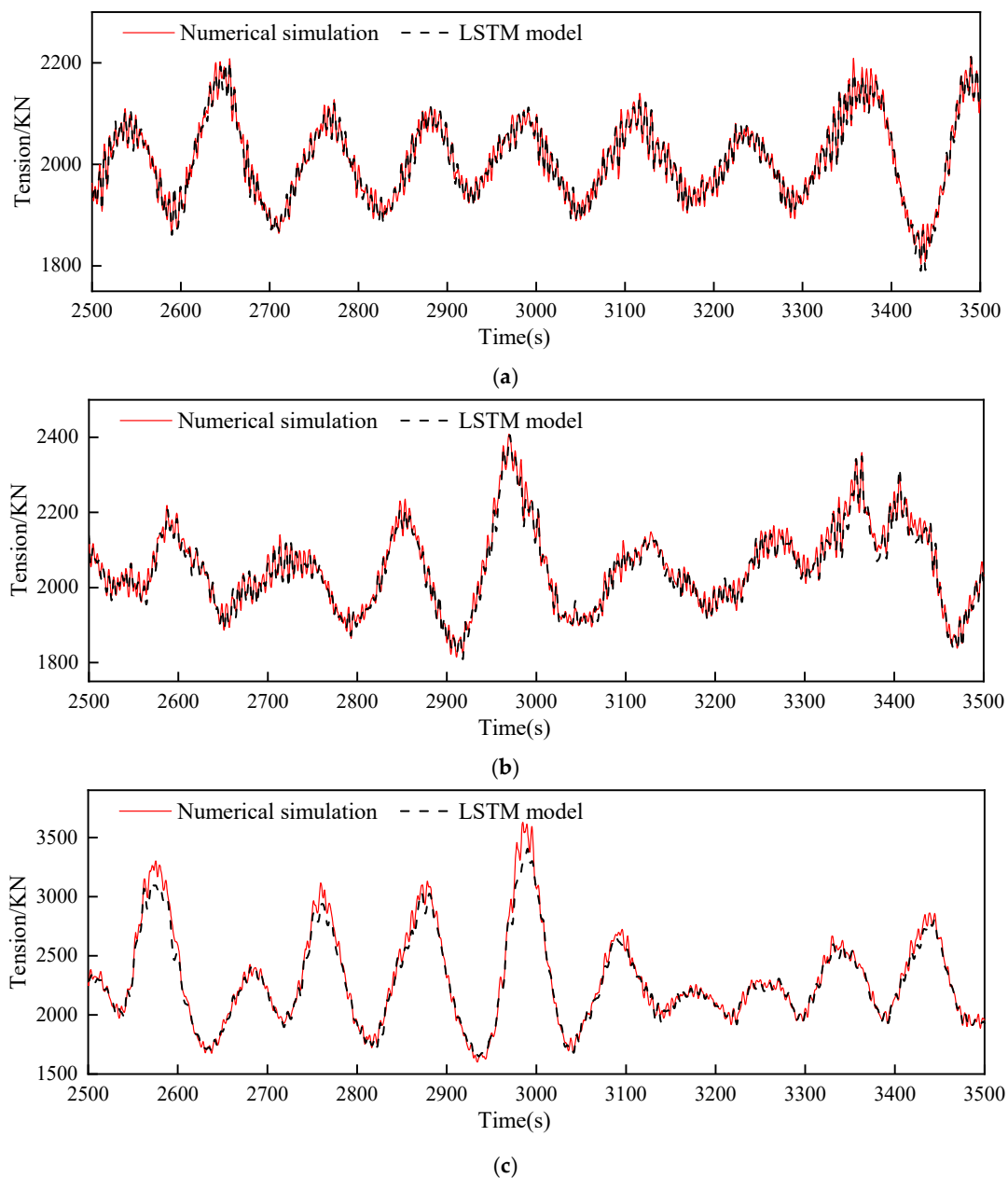


Figure 9. Cont.

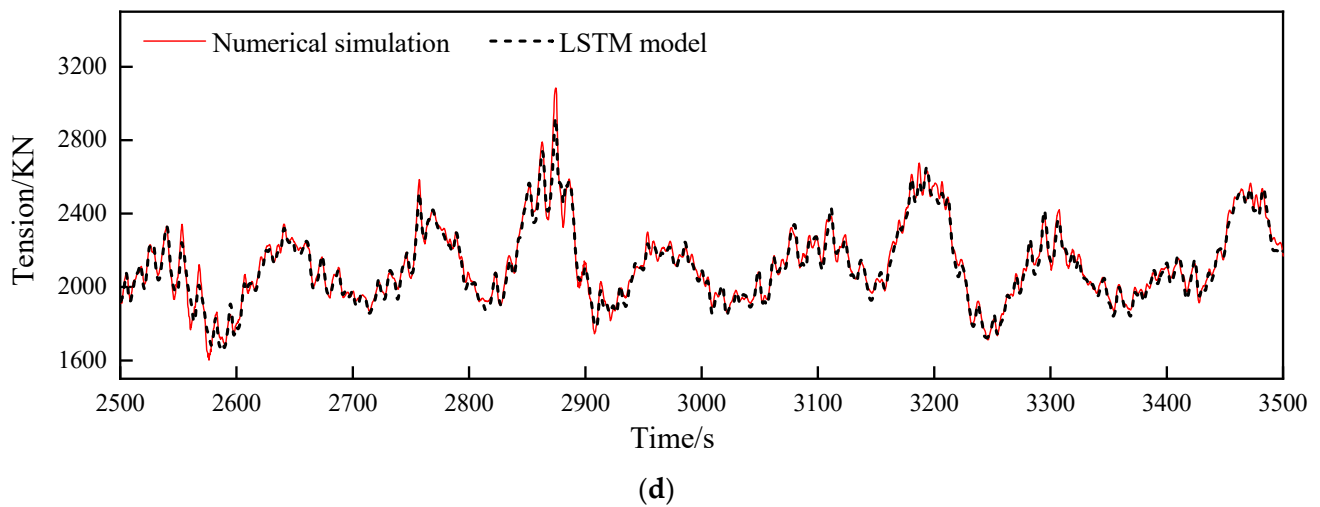


Figure 9. Comparison of prediction results under sea state 4–7 (line #1). (a) Tension time series prediction of line #1 under sea state 4; (b) tension time series prediction of line #1 under sea state 5; (c) tension time series prediction of line #1 under sea state 6; and (d) tension time series prediction of line #1 under sea state 7.

From the comparison of predicted time series (Figure 9), it can be seen that the variation trend of the top tension series predicted by the LSTM model is basically consistent with the calculation results and there is no obvious deviation in the phase of the predicted time series. But when the tension grows rapidly, the prediction error also increases significantly, especially at extreme points. As shown in Figure 9, the tension of line #1 under sea state 6 gets increased sharply during 2900–3000 s, and the predicted tension is obviously lower than the numerical simulation result at the peak. It is because when the tension changes rapidly, the nonlinearity of the mooring system also gets enhanced. The prediction performance of the LSTM model is affected by the local strong nonlinearity phenomenon, which leads to the decrease of the prediction accuracy.

From the comparison of statistical errors, as shown in Figure 10 and Table 5, it is notable that most of the prediction errors of the maximum tension are within 5 % except for line 1 under sea state 6. The fluctuation of the prediction results is due to the change of the internal weight matrix of the deep learning model during the training process, but the overall prediction error E_{max} is less than 6 %, which can preliminarily verify the prediction accuracy of the proposed model. Table 5 shows the RMSE of the prediction results of the whole time series. It can be seen that the value of RMSE is relatively small compared with the overall range of the tension, which means that the model can achieve good prediction performance for the whole time series in sea states 4–7.

Table 5. The RMSE of prediction results under sea states 4–7.

Sea State	RMSE (KN)			
	Line #1	Line #2	Line #3	Line #4
4	9.285	5.541	5.937	9.663
5	23.318	10.359	11.557	17.981
6	49.219	26.351	24.313	40.752
7	44.055	23.632	21.157	27.602

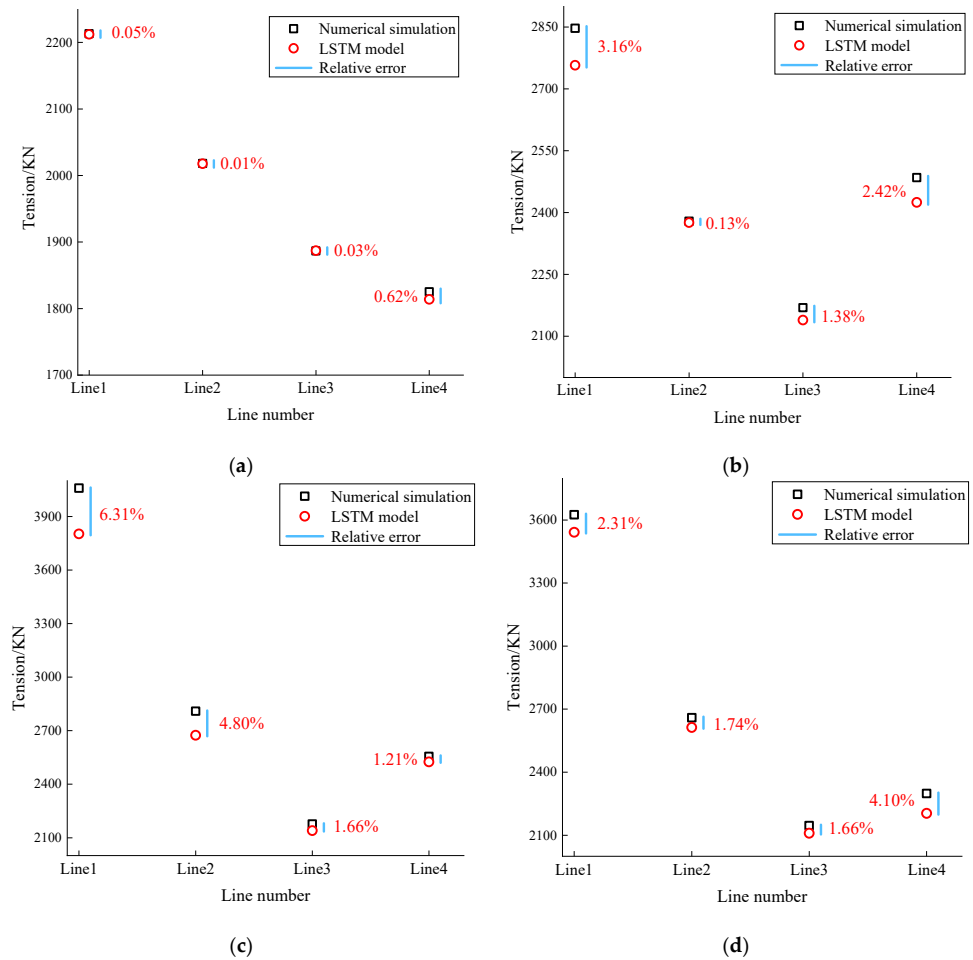


Figure 10. Comparison of the E_{max} of mooring lines under sea state 4–7. (a) Sea state 4; (b) sea state 5; (c) sea state 6; and (d) sea state 7.

6.3. The Effect of Data Skewness on Prediction Accuracy

The raw data can be well transformed to the normal distribution through the Box-Cox Transformation (BCT). Figure 11 shows the data distribution of line 1 in sea state 7 before and after the BCT. It can be seen that the mooring load data becomes a symmetrical distribution after the BCT and the skewness is decreased from 1.274 to 0.101.

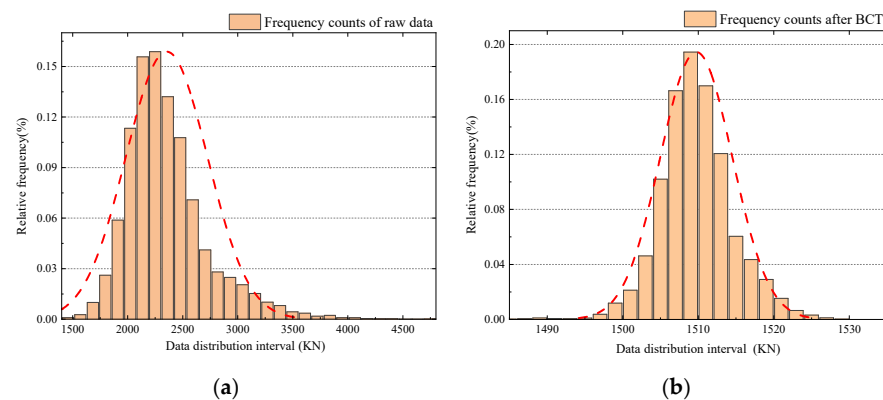


Figure 11. The comparison of data distribution between the raw data and transformed data. (a) Frequency counts of the raw data (skewness = 1.274); (b) frequency counts after the BCT (skewness = 0.101).

To further study the effect of data skewness on the model prediction accuracy, this paper applies the skewness processing method proposed in Section 4.3. We have investigated the improvement of the prediction accuracy under different sea conditions. The mooring load prediction results of line 1 in sea state 4–7 are detailed and analyzed in this section. The corresponding comparison results and statistical errors are displayed in Figure 12 and Table 6. To observe the prediction performance at the maximum point conveniently, the detailed partial enlarged view is set for comparative analysis.

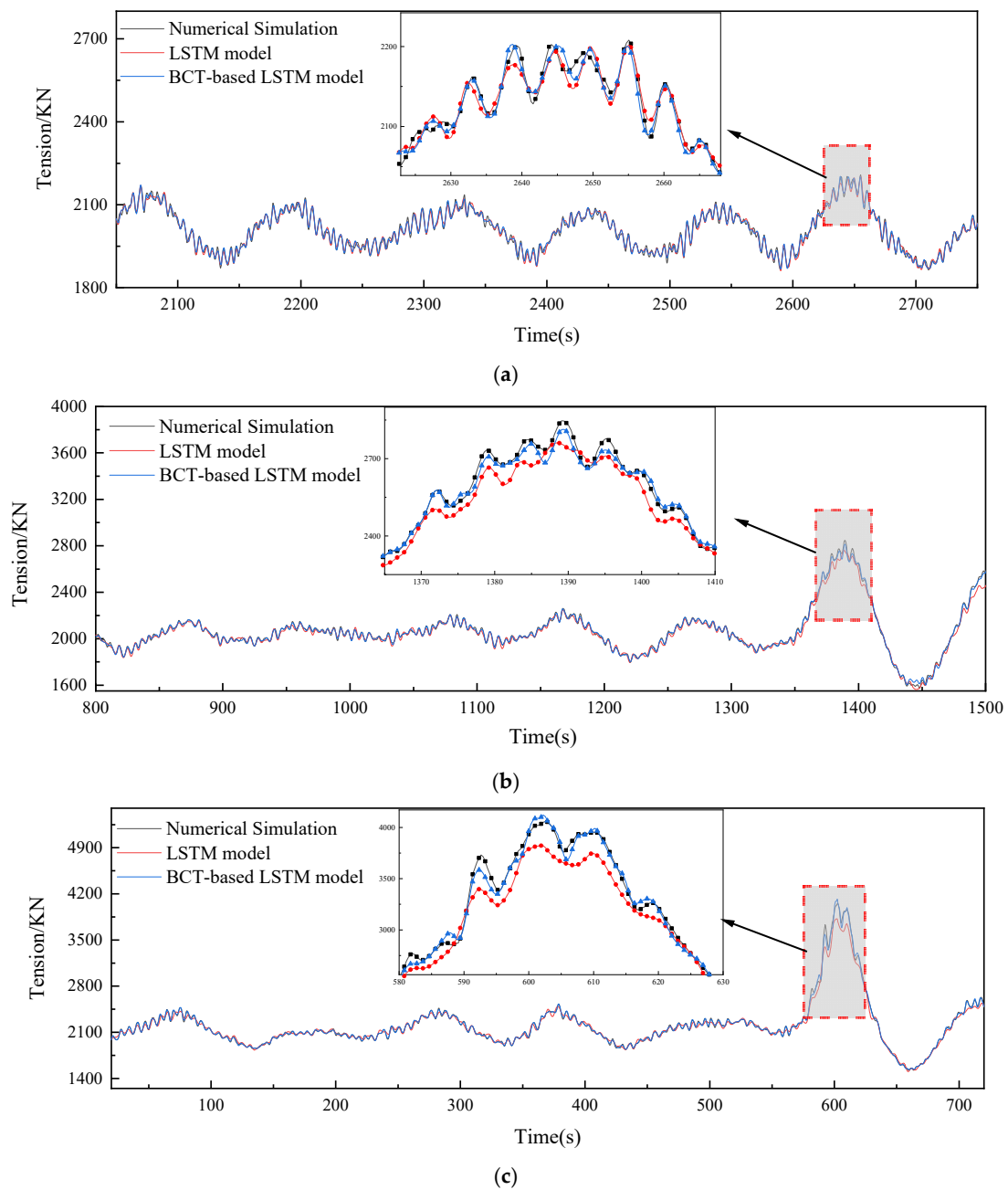


Figure 12. Cont.

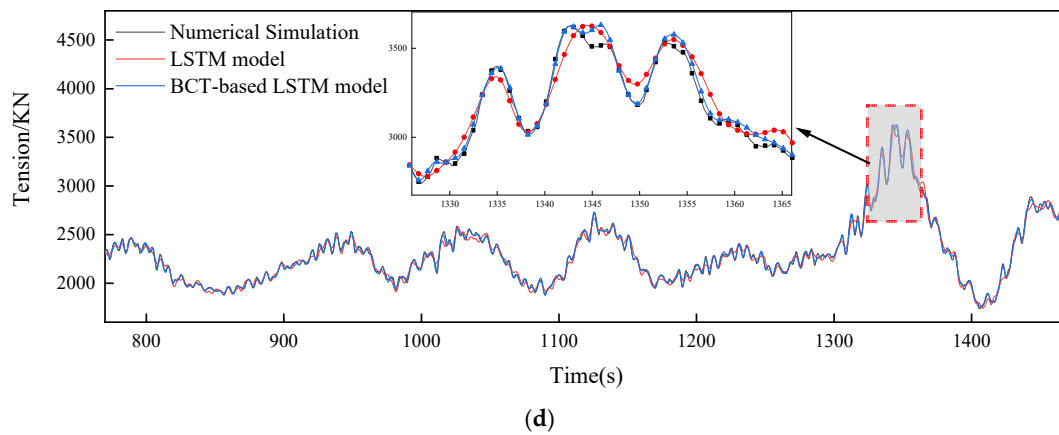


Figure 12. The comparison of prediction results under sea state 4–7. (a) The comparison of prediction results under sea state 4; (b) the comparison of prediction results under sea state 5; (c) the comparison of prediction results under sea state 6; and (d) the comparison of prediction results under sea state 7.

Table 6. The statistical error of line 1 under sea states 4–7.

Sea State	Skewness	E_{max}		RMSE (KN)		Improvement Ratio
		LSTM Model	BCT-Based LSTM Model	LSTM Model	BCT-Based LSTM Model	
4	0.108	−0.05%	0.02%	9.29	7.45	19.78%
5	0.666	−3.16%	−1.19%	23.32	9.71	58.37%
6	1.148	−6.31%	1.15%	49.22	14.60	70.33%
7	1.274	−2.31%	0.05%	44.05	20.72	52.96%

Improvement ratio: The ratio reflects the improvement of the BCT-based LSTM model (BLM) over the LSTM model (LM) on the prediction accuracy, which is calculated by $\frac{RMSE_{LM} - RMSE_{BLM}}{RMSE_{LM}} \times 100\%$.

From the comparison of predicted time series (Figure 12), it can be seen that under the low sea state with small data skewness, the prediction performance between the LSTM model and the BCT-based model are close. With the increase of sea state and data skewness, the prediction accuracy of two models has shown significant difference. Taking the prediction results under sea state 6 as an example (Figure 12c), the predicted mooring load variation curve by the BCT-based LSTM model is more consistent with numerical simulation results. Meanwhile, during 600–610 s, the BCT-based LSTM model shows greater fitting performance for extreme points.

From the comparison of statistical errors, as shown in Figure 13 and Table 6, it is notable that after the Box-Cox Transformation, the E_{max} of prediction results are all within 1.5% and the RMSE are reduced to less than 25 KN under all sea states. Considering the data skewness under sea state 4–7, it can be found that when the data is in the symmetrical distribution with small skewness, the BCT method has little improvement on the prediction accuracy, which is only 19.78%. However, if the mooring load data is in moderate asymmetry or high asymmetry, the preprocessing of data skewness will significantly improve the prediction performance of the LSTM model, which are more than 50%. That is because during the training process, the LSTM model performance is determined by the selected data. As shown in Graph a, Figure 11, when training the model by the raw data, the neural network will extract more data features near the mode of the data, which is in the range of 2000–2500 KN. For the maximum values of the mooring load data in the range of 3500–4000 KN, the training effect of the model will be poor and resulting in the obvious deviation of prediction results at these extreme points. Thus, when the data follows the normal distribution and the extreme points are well distributed among the dataset, the LSTM model can be fully trained and effectively improve the prediction accuracy.

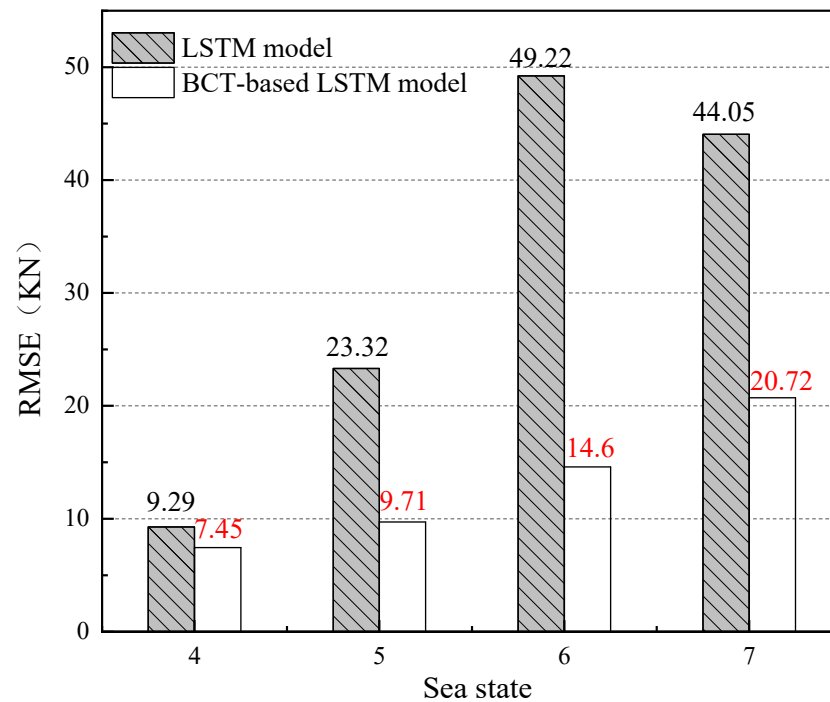


Figure 13. The comparison of RMSE of prediction results.

7. Conclusions

Deep learning methods have unique advantages in dealing with nonlinear problems. There is an obvious non-linear relationship between the motion of the deep-sea platform and the load response of the mooring lines. Therefore, it is significant to carry out the research of predicting the mooring load based on the platform motion through the deep learning method. Meanwhile, the mooring load shows different data distribution characteristics under various sea conditions. Analyzing the data characteristics and using appropriate preprocessing methods can effectively improve the prediction accuracy of the model.

In this paper, a LSTM-based mooring load prediction model is constructed, which takes the platform motion as input and mooring load as output. The numerical simulation results of a deep-water semi-submersible platform are employed as the data source. Based on the simulated results, this paper mainly studies the distribution characteristics of the mooring load data under different sea states and further investigates the influence of data skewness on prediction performance. A data preprocessing method based on the Box-Cox Transformation is proposed to improve prediction accuracy. According to the results in this study, the following conclusions can be drawn:

First, the performance of the constructed LSTM-based mooring load prediction model is preliminarily verified by numerical simulation results. The tension time series predicted by the LSTM model can maintain great consistency of the simulation results under sea states 4–7 and the E_{\max} are all within 6%. However, there are still some obvious deviations between the comparison results, especially at some maximum points.

Second, the data distribution characteristics of mooring load under sea states 4–7 are analyzed. The results show that with the increase of sea states, the corresponding data skewness also increases. The data gradually deviates from the normal distribution, which changes from symmetrical distribution to asymmetry.

Finally, the effect of the proposed data skewness processing method is verified under sea states 4–7. After the Box-Cox Transformation, the prediction performance at maximum points are obviously improved compared with the original LSTM-based model. The E_{\max} of prediction results are all within 1.5% and the RMSE are reduced to less than 25 KN under

all sea states. The above comparison results can fully indicate that reducing the mooring load data skewness can effectively improve the prediction accuracy of the LSTM model.

Author Contributions: Conceptualization, L.H. and H.C.; methodology, K.Z. and H.C.; software, H.C.; validation, W.H.; formal analysis, Y.B. and K.Z.; investigation, L.H. and Y.B.; writing—original draft preparation, H.C.; writing—review and editing, W.H. and K.Z.; visualization, W.H. All authors have read and agreed to the published version of the manuscript.

Funding: The present work is sponsored by the high-level scientific research guidance special cross-innovation support plan of Harbin Engineering University (No. 3072022JC0102) and the Domain Foundation of Equipment Advance Research, China (Grant No. 80907020801).

Institutional Review Board Statement: Not applicable.

Informed Consent Statement: Not applicable.

Data Availability Statement: All data, models, or code generated or used during the study are available from the corresponding author by request.

Acknowledgments: The authors would like to thank the members of Wenyang Duan's research team at Harbin Engineering University for their careful guidance.

Conflicts of Interest: The authors declare no conflict of interest.

References

1. Lv, J.; Guo, X.; Yang, J. Development status and trend of deepwater oil-gas exploration and development technology. *Oil Drill. Prod. Technol.* **2015**, *37*, 13–18.
2. Leonard, J.W. Nonlinear Dynamics of Cables with Low Initial Tension. *J. Eng. Mech. Div.* **1972**, *98*, 293–309. [[CrossRef](#)]
3. Webster, R. Nonlinear static and dynamic response of underwater cables structures using the finite element method. In Proceedings of the Offshore Technology Conference, Houston, TX, USA, 4 May 1975; Volume 2, pp. 754–764.
4. Lindahl, J.; Sjoberg, A. Dynamic analysis of mooring cables. In Proceedings of the Second International Symposium on Ocean Engineering and Ship Handling, Gothenburg, Sweden, 1–3 March 1983; pp. 281–319.
5. Sagrilo, L.V.S.; Siqueira, M.Q.; Ellwanger, G.B.; Lima, E.C.P.; Ribeiro, E.J.B.; Lemos, C.A.D. On the extreme response of heave-excited flexible risers. *Appl. Ocean. Res.* **2000**, *22*, 225–239. [[CrossRef](#)]
6. Pascoal, R.; Huang, S.; Barltrop, N.; Guedes Soares, C. Equivalent force model for the effect of mooring systems on the horizontal motions. *Appl. Ocean. Res.* **2005**, *27*, 165–172. [[CrossRef](#)]
7. Gobat, J.I.; Grosenbaugh, M.A. A simple model for heave-induced dynamic tension in catenary moorings. *Appl. Ocean. Res.* **2001**, *23*, 159–174. [[CrossRef](#)]
8. Li, M.; Tian, G.; Li, D.; Li, P. The quick forecasting method of mooring load based on the frequency domain analysis. *Ship Ocean. Eng.* **2017**, *46*, 34–36.
9. Liu, H.F.; Bi, C.W.; Zhao, Y.P. Experimental and numerical study of the hydrodynamic characteristics of a semisubmersible aquaculture facility in waves. *Ocean. Eng.* **2020**, *214*, 107714. [[CrossRef](#)]
10. Akita, R.; Yoshihara, A.; Matsubara, T.; Uehara, K. Deep learning for stock prediction using numerical and textual information. In Proceedings of the 2016 IEEE/ACIS 15th International Conference on Computer and Information Science (ICIS), IEEE, Okayama, Japan, 26–29 June 2016; pp. 1–6.
11. Pan, W.; Chen, D. Research on short-term traffic flow prediction based on GRU-SVR. *Comput. Technol. Dev.* **2019**, *29*, 11–14.
12. Zheng, Y.; Wang, H. Study on short-term road traffic flow prediction based on deep learning. *Comput. Eng. Softw.* **2020**, *41*, 72–74.
13. Mazaheri, S.; Mesbahi, E.; Downie, M.J.; Incecik, A. Seakeeping analysis of a turret-moored FPSO by using artificial neural networks. In Proceedings of the OMAE 2003—22nd International Conference on Offshore Mechanics and Arctic Engineering, Cancun, Mexico, 8–13 June 2003.
14. Mazaheri, S.; Downie, M.J. Response-based method for determining the extreme behaviour of floating offshore platforms. *Ocean. Eng.* **2004**, *32*, 363–393. [[CrossRef](#)]
15. Guarize, R.; Matos, N.A.F.; Sagrilo, L.V.S.; Lima, E.C.P. Neural networks in the dynamic response analysis of slender marine structures. *Appl. Ocean. Res.* **2007**, *29*, 191–198. [[CrossRef](#)]
16. de Pina, A.C.; de Pina, A.A.; Albrecht, C.H.; de Lima, B.S.L.P.; Jacob, B.P. ANN-based surrogate models for the analysis of mooring lines and risers. *Appl. Ocean. Res.* **2013**, *41*, 76–86. [[CrossRef](#)]
17. Sagrilo Luis, V.S.; de Sousa Fernando, J.M.; Cortina Joao, P.R. Neural Networks Applied to the Wave-Induced Fatigue Analysis of Steel Risers. *Math. Probl. Eng. Theory Methods Appl.* **2018**, *2018 Pt 9*, 2719682.1–2719682.16.
18. Murat, Y.; Yooil, K. Time series prediction of mooring line top tension by the NARX and Volterra model. *Appl. Ocean. Res.* **2019**, *88*, 170–186.
19. Zhao, Y.P.; Bi, C.W.; Sun, X.X.; Dong, G.H. A Prediction on Structural Stress and Deformation of Fish Cage in Waves Using Machine-Learning Method. *Aquac. Eng.* **2019**, *85*, 15–21. [[CrossRef](#)]

20. Bi, C.W.; Zhao, Y.P.; Sun, X.X.; Zhang, Y.; Guo, Z.X.; Wang, B.; Dong, G.H. An efficient artificial neural network model to predict the structural failure of high-density polyethylene offshore net cages in typhoon waves. *Ocean. Eng.* **2020**, *196*, 106793. [[CrossRef](#)]
21. Hou, J.; Qi, Y. On the Prediction in Time Domain of Ship Non-Stationary Swaying Motions. In Proceedings of the 3rd International Conference on Information Technology and Computer Science, Huangshi, China, 23–24 July 2011; American Society of Mechanical Engineers: New York, NY, USA, 2011.
22. Duan, W.Y.; Han, Y.; Huang, L.M.; Zhao, B.B.; Wang, M.H. A hybrid EMD-SVR model for the short-term prediction of significant wave height. *Ocean. Eng.* **2016**, *124*, 54–73. [[CrossRef](#)]
23. Zihan Chang Zhang, Y.; Chen, W. Electricity price prediction based on hybrid model of adam optimized LSTM neural network and wavelet transform. *Energy* **2019**, *187*, 115804.
24. De Pina, A.C.; Albrecht, C.H.; De Lima, B.S.L.P.; Jacob, B.P. Wavelet network meta-models for the analysis of slender offshore structures. *Eng. Struct.* **2014**, *68*, 71–84. [[CrossRef](#)]
25. De Pina, A.C.; Monteiro, B.F.M.; Albrecht, C.H.; De Lima, B.S.L.P.; Jacob, B.P. ANN and wavelet network meta-models for the coupled analysis of floating production systems. *Appl. Ocean. Res.* **2014**, *48*, 21–32. [[CrossRef](#)]
26. Sidarta, D.E.; Kyoung, J.; O’Sullivan, J.; Lambrakos, K.F. Prediction of offshore platform mooring line tensions using artificial neural network. In Proceedings of the ASME 36th International Conference on Ocean, Offshore and Arctic Engineering, Trondheim, Norway, 25–30 June 2017.
27. Qiao, D.; Li, P.; Ma, G.; Qi, X.; Yan, J.; Ning, D.; Li, B. Realtime prediction of dynamic mooring lines responses with LSTM neural network model. *Ocean. Eng.* **2021**, *219*, 108368. [[CrossRef](#)]
28. Jing, X.; Webster, W.C.; Xu, Q.; Lambrakos, K. Coupled Dynamic Modeling of a Moored Floating Platform with Risers. In Proceedings of the ASME 2011 30th International Conference on Ocean, Offshore and Arctic Engineering, Rotterdam, The Netherlands, 19–24 June 2011.
29. Hochreiter, S.; Schmidhuber, J. Long Short-Term Memory. *Neural Comput.* **1997**, *9*, 1735–1780. [[CrossRef](#)] [[PubMed](#)]
30. Pearson, K. Contributions to the mathematical theory of evolution. *Philos. Trans. Roy. Soc. Lond. A Math. Phys. Sci.* **1894**, *185*, 71–110.
31. Groeneveld, R.A.; Meeden, G. Measuring skewness and kurtosis. *J. Roy. Stat. Soc. D* **1984**, *33*, 391–399. [[CrossRef](#)]
32. Rayner, J.C.W.; Best, D.J.; Mathews, K.L. Interpreting the skewness coefficient. *Commun. Statist. Theory Methods* **1995**, *24*, 593–600. [[CrossRef](#)]
33. Ma, S.; Duan, W.Y.; Han, X.L. Dynamic Asynchronous Coupled Analysis and Experimental Study for a Turret Moored FPSO in Random Seas. *J. Offshore Mech. Arct. Eng.* **2015**, *137*, 41302. [[CrossRef](#)]
34. Chen, J.K.; Wang, H.; Ma, S.; Wang, L.J. Hydrodynamic calculation and analysis on a semi-submersible platform based on Taylor expansion boundary element method. *J. Harbin Eng. Univ.* **2018**, *39*, 1431–1437.